Brazilian Journal of Microbiology (2023) 54:53–68
https://doi.org/10.1007/s42770-022-00875-2

BACTERIAL, FUNGAL AND VIRUS MOLECULAR BIOLOGY - RESEARCH PAPER

Integrative transcriptome analysis of SARS-CoV-2 human-infected cells combined with deep learning algorithms identifies two potential cellular targets for the treatment of coronavirus disease

Ricardo Lemes Gonçalves[1] · Gabriel Augusto Pires de Souza[2,3] · Mateus de Souza Terceti[2] · Renato Fróes Goulart de Castro[2] · Breno de Mello Silva[1] · Romulo Dias Novaes[4] · Luiz Cosme Cotta Malaquias[2] · Luiz Felipe Leomil Coelho[2]

Received: 29 January 2022 / Accepted: 14 November 2022 / Published online: 26 November 2022

Abstract

Severe acute respiratory syndrome coronavirus 2 (SARS-CoV-2) quickly spread worldwide, leading coronavirus disease 2019 (COVID-19) to hit pandemic level less than 4 months after the first official cases. Hence, the search for drugs and vaccines that could prevent or treat infections by SARS-CoV-2 began, intending to reduce a possible collapse of health systems. After 2 years, efforts to find therapies to treat COVID-19 continue. However, there is still much to be understood about the virus' pathology. Tools such as transcriptomics have been used to understand the impact of SARS-CoV-2 on different cells isolated from various tissues, leaving datasets in the databases that integrate genes and differentially expressed pathways during SARS-CoV-2 infection. After retrieving transcriptome datasets from different human cells infected with SARS-CoV-2 available in the database, we performed an integrative analysis associated with deep learning algorithms to determine differentially expressed targets mainly after infection. The targets found represented a fructose transporter (GLUT5) and a component of proteasome 26s. These targets were then molecularly modeled, followed by molecular docking that identified potential inhibitors for both structures. Once the inhibition of structures that have the expression increased by the virus can represent a strategy for reducing the viral replication by selecting infected cells, associating these bioinformatics tools, therefore, can be helpful in the screening of molecules being tested for new uses, saving financial resources, time, and making a personalized screening for each infectious disease.

Keywords Integrative bioinformatic · Integrative transcriptome analysis · SARS-CoV-2 · COVID-19 · Deep learning · Emerging virus disease

Introduction

Coronaviruses belong to a family of enveloped RNA viruses of medical and veterinary importance, which have recently induced several outbreaks worldwide and caused fatal respiratory diseases in humans [1, 2]. The severe acute respiratory

Ricardo Lemes Gonçalves and Gabriel Augusto Pires de Souza contributed equally to this work and shared authorship.

Responsible Editor: Luis Nero

✉ Luiz Felipe Leomil Coelho
luiz.coelho@unifal-mg.edu.br

[1] Núcleo de Pesquisas em Ciências Biológicas, NUPEB, Universidade Federal de Ouro Preto, Ouro Preto 35400-000, Brazil

[2] Laboratório de Vacinas, Departamento de Microbiologia e Imunologia, Instituto de Ciências Biomédicas, Universidade Federal de Alfenas, Rua Gabriel Monteiro da Silva, 700, 37130-001 Alfenas, Brazil

[3] Laboratório de Vírus, Departamento de Microbiologia, Instituto de Ciências Biológicas, Universidade Federal de Minas Gerais, Av. Antônio Carlos, 6627, Belo Horizonte 31270-901, Brazil

[4] Instituto de Ciências Biomédicas, Departamento de Biologia Estrutural, Universidade Federal de Alfenas, Alfenas, Minas Gerais, Brazil

coronavirus syndrome (SARS-CoV) that emerged in 2002 [3] and the Middle East respiratory syndrome coronavirus (MERS-CoV) of 2012 [4, 5] are examples of two highly pathogenic coronaviruses with zoonotic origin.

In late 2019, a new highly transmissible coronavirus called SARS-CoV-2 emerged in China, beginning an outbreak of viral pneumonia known as coronavirus disease 2019 (COVID-19) that spread rapidly around the world configuring itself as a pandemic [6–8]. SARS-CoV-2 overwhelmingly surpassed SARS and MERS in terms of the number of infected people and the spatial breadth of epidemic areas. As a new beta-coronavirus SARS-CoV-2 shares 79% genome sequence identity with SARS-CoV and 50% with MERS-CoV [9].

The World Health Organization (WHO) has confirmed more than 630 million cases of COVID worldwide, including about 6.5 million deaths [8]. Thus, the ongoing outbreak of COVID-19 represents an extraordinary threat to the world's public health [10–13]. Although several studies have shown that certain drugs may bring some benefits in patients' subpopulations, there are few effective therapies for COVID-19 or antivirals against SARS-CoV-2.

The drugs tested so far can act by preventing the entry of SARS-CoV-2 into the cell [14–19], directly inactivating viral replication [20–24], or acting as immunomodulating agents to reduce the excessive inflammatory response [25–30]. However, despite the anti-virus drugs and immunomodulators tested so far, it is clear that vaccination is the most effective long-term strategy for prevention and control [2].

Furthermore, the molecular mechanisms of pathogenesis of SARS-CoV-2 and virus–host interactions infection remain primarily unclear [2]. In this sense, omics technologies, especially transcriptome studies, can generate thousands of information about the gene regulation process in host cells after infection by a virus and, therefore, can help obtain relevant data on pathogenesis and pathogen–host interaction[31, 32].

Thus, the in silico integrative transcriptome analysis (ITA) has proven to be a promising approach for understanding biological events in complex diseases [33]. It can connect different data sources, reduce complexity, and increase data's predictive value through unified systems. Therefore, identifying the altered expression profile by ITA can contribute to understanding the virus pathogenesis and the development of new antiviral drugs, as performing joint and integrated analysis of several transcriptomes [34]. In addition, ITA has been used to find genes with significant associations for neurodegenerative disease (Alzheimer), cancer, and emerging viral disease (Zika) [33–40].

Therefore, this study aimed to perform an integrative analysis of transcriptomes from SARS-Cov-2-infected cells to identify genes and biological pathways essential for understanding the pathogenesis and identifying therapeutic strategies for COVID-19. Here, we show that a combination of ITA and highly efficient structural modeling through the breakthrough advance of deep learning algorithms can identify shared differentially expressed genes (DEGs) between SARS-CoV-2-infected cells. Furthermore, structural bioinformatics analysis confirms the potential drug–gene interaction of two DEGs (SLC2A5 and PSMD2). Therefore, the proposed in silico protocol performed can predict and identify putative cellular proteins that can be useful to guide the identification of candidate antiviral drugs or repurposing drugs to treat SARS-CoV-2.

Methods

The transcriptome of cells infected with SARS-CoV-2

Gene expression profiling data from SARS-CoV-2-infected human cells were retrieved from RNA sequencing data from the Gene Expression Omnibus platform (https://www.ncbi.nlm.nih.gov/gds). The platform was extensively searched for datasets of any human cell infected with SARS-COV-2. Information about the cell type used, the multiplicity of infection (MOI), time of infection, and sequencing platform were represented in Table 1. The raw sequence data were accessed using the online Galaxy platform (https://usegalaxy.org/), and the identification of differentially expressed genes (DEG) were obtained using the "Tuxedo suite" protocol as described in Pires de Souza and colleagues (2020). Only datasets that were performed with at least two replicates for each experimental sample were considered for the analysis. The final DEG list was identified from each study to fulfill an integrative analysis.

Network construction

All networks were built using the Gephi software version 0.9.2 [41]. The cells and genes were listed in a comma-separated values (.csv) spreadsheet for each graph, and this file was imported into the software. Another.csv spreadsheet with the connections between the cells and genes was also imported to generate the network graphs. The node diameter is directly proportional to the edge in all networks. The layout was generated using algorithms based on the force of attraction and repulsion of the nodes (Force Atlas 2). Finally, the nodes were submitted to local rearrangement to better visualize the connections between nodes.

Molecular modeling and validation of SLC2A5 and PSMD2 isoform structures

The three-dimensional models of isoform 1 of SLC2A5 (id: P22732) and PSMD2 (ID: Q13200) were generated from the AlphaFold database (https://alphafold.ebi.ac.uk/)

Table 1 Summary of datasets and sample details

GEO access	Cell type	SARS-COV-2 strain	MOI	Time of infection	NGS platform
GSE150392	Cardiomyocyte	USA-WA1/2020	0.1	72 h	Illumina NextSeq 500
GSE148729	Caco2	NR	0.3	24 h	Illumina NextSeq 500 Illumina HiSeq 4000
GSE148729	Calu3	NR	0.3	24 h	Illumina NextSeq 500 Illumina HiSeq 4000
GSE148729	HT199	NR	0.3	24 h	Illumina NextSeq 500 Illumina HiSeq 4000
GSE153970	Primary human airway epithelial cell (hEC)	USA-WA1/2020	0.25	48 h	Illumina NovaSeq 6000
GSE154613	A459 cells expressing human ACE2	USA-WA1/2020	0.2	24 h	Illumina NextSeq 500
GSE150728	Peripheral blood mononuclear cells*	—	—	—	Illumina NovaSeq 6000

NR, not reported

ACE2, angiotensin I-converting enzyme-2

NGS, next-generation sequencing

*Cells isolated from COVID-19 patients

partnership between DeepMind and EMBL-EBI, which set out to solve all the main protein structures encoded by the human genome through the new tool based on deep learning, AlphaFold2 [42], responsible for a "breakthrough advance" of protein modeling in CASP14. However, the structure of PSMD2 isoform 1 was considered unfeasible for the present study due to the low quality of the sizeable N-terminal portion of the polypeptide chain (data not shown). Furthermore, the AlphaFold Database does not present any other known isoforms for the modeled proteins. Therefore, isoform 2 (ID: P22732-2) of SLC2A5 and isoforms 1 and 2 (ID: Q13200-2) and 3 (ID: Q13200-3) of PSMD2 were generated through the Robetta Server (https://robetta.bakerlab. org/) using the RobettaAFold algorithm [43], which is based on the same deep learning method used by AlphaFold2. From the models generated for each structure, those with the best quality were selected and verified through the MolProbity score [44].

Those generated models were submitted to structural refinement simulation through the GalaxyRefine [45] server (http://galaxy.seoklab.org/cgi-bin/submit.cgi?type=REFINE), which provided different refined models, being the structures with the highest quality selected for the job. Finally, the final models' quality was validated through the Prosa-web [46] servers (https://prosa.services.came.sbg.ac.at/prosa.php) which compares the quality of the targets as a function of their total energy distributions. Target structure with the protein structures experimentally resolved by X-ray diffraction and nuclear magnetic resonance. Also used to check the quality of individual models, the MolProbity server (http://molprobity.biochem.duke.edu/) provided MolProbity score that combines different structural parameters to provide a normalized score, favoring the comparison of models with experimentally solved structures and, lastly, the individual construction of Ramachandran plot.

Preparation of receptors and ligands

The amino acid residues of SLC2A5 and PSMD2 isoforms received charges and polar hydrogens. Later, the models were aligned and had their structural centers determined. A grid box was delimited from these, completely covering each MGLTools (Morris et al., 2009) model. The coordinates and box sizes were *X*, 13,153, 64; *Y*, 33,099, 76; and *Z*, − 18,273, 54, for the structures of SLC2A5 and *X*, 1703, 80; *Y*, 43,775, 92; and *Z*, 38,746, 108, for PSMD2. Potential ligands for SLC2A5 had their structures obtained through PubChem: glufosfamide (CID: 123,628) and streptozocin (CID29327). In addition, D-fructose (ChEBI: 37,721) was used as the substrate of the isoforms of SLC2A5, and fludeoxyglucose (18F) (CID: 68,614) was used as an inhibitor. Potential ligands for PSMD2 were also obtained from PubChem (bortezomib (CID: 387,447), carfilzomib (CID: 11,556,711), ixazomib citrate (CID: 56,844,015), and oprozomib (CID: 25,067,547)). All composite structures had their torsions and charges, and hydrogens were added by Open Babel. The blind molecular docking's independent simulations were performed using Vina software [47] using exhaustiveness 32. Finally, the result of the simulations was analyzed and visualized using BIOVIA Discovery Studio® and Pymol software [48].

Results

Differentially expressed genes on SARS-CoV-2-infected cells

As illustrated in Fig. 1, a seven-step bioinformatic approach was used to identify candidate genes that could be targeted for antiviral development compounds against SARS-CoV-2. The search for transcriptome studies of human cells

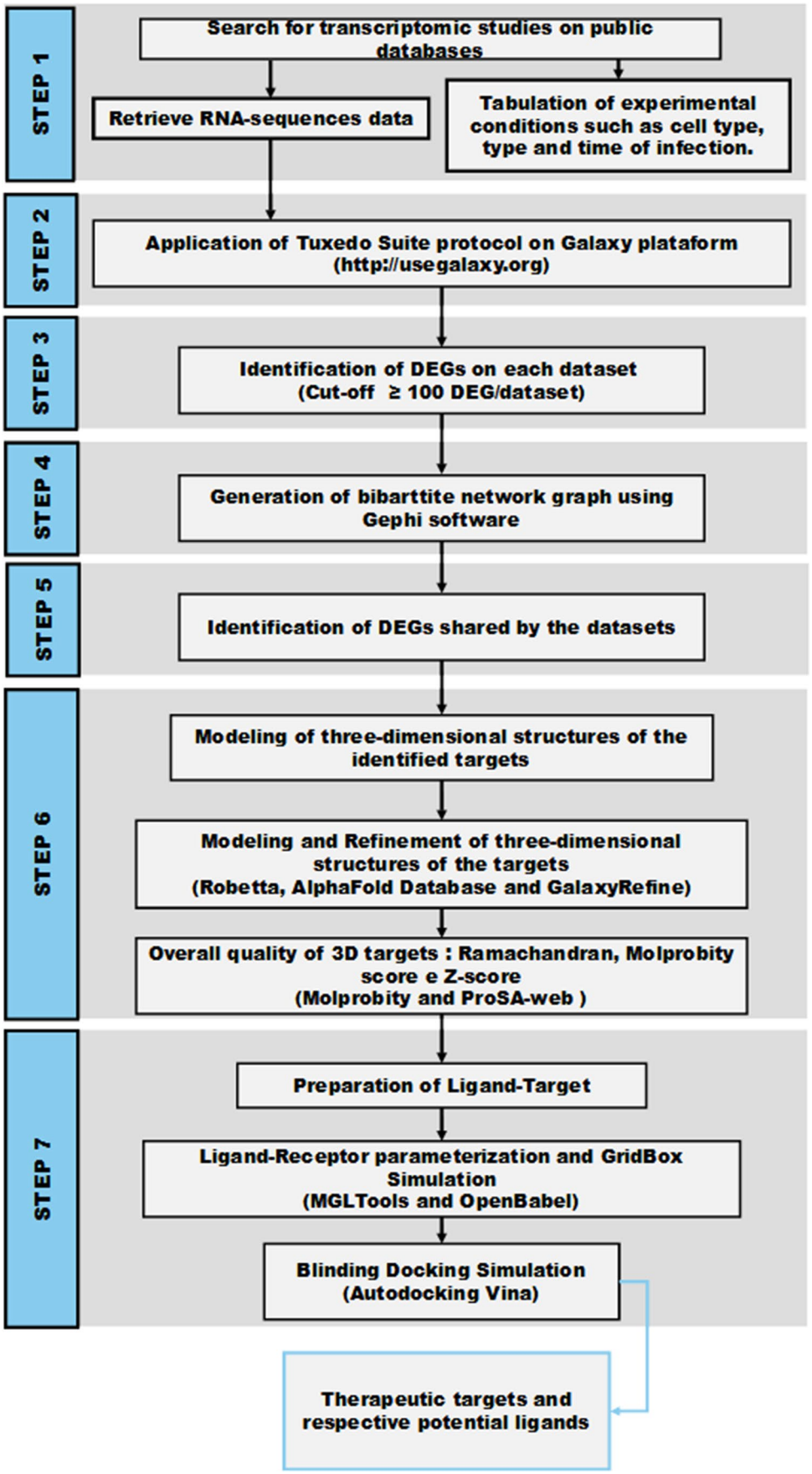

Fig. 1 Schematic representation of the entire in silico approach for identifying potential targets for the treatment of coronavirus disease

infected with SARS-CoV-2 resulted in the selection of 7 datasets. All experimental data, such as time of infection, cell type, SARS-CoV-2 strain, the multiplicity of infection (MOI), GEO number access, and sequencing platform, were described in Table 1. Several cell types were used in these experiments, such as cells derived from cardiovascular (cardiomyocyte), epidermal (HT199 melanoma cells), intestinal (Caco2), pulmonary (Calu3, primary human airway epithelial cells, A459), and immune systems (peripheral blood mononuclear cells). Tuxedo suite protocol was performed based on the transcriptome data from each study to understand better the changes in gene expression in each cell type after SARS-CoV-2 infection. Table 2 shows the number of differentially expressed genes (DEG) with statistical significance identified in each study.

Interaction networks between DEGs and cells were built from the identification of differentially expressed genes in each study. As shown in Fig. 2, there is a cell-specific gene expression profile since few differentially expressed genes were common to different cell types. Few genes were shared between two distinct cells (339/4.18%) and one of three cell types (7/0.08%). No DEG was shared between four or more cell types (Fig. 3). Table 3 represents the DEGs that were shared between three cell types. DEGs that had their expression increased after SARS-COV-2 infection are chosen for molecular docking analysis. The increase in their expression may be related to a dependence on the molecular function of the proteins encoded by these genes in the replication cycle of SARS-CoV-2.

Once the differentially expressed genes in three cell types were identified, the search for drugs that could directly interact with the proteins encoded by these genes began, using the DGIdb 3.0 platform (Wagner ET AL., 2018). The results obtained demonstrate that only the SLC2A5, PSMD2, and GNB3 genes presented drugs with the potential to interact with the proteins encoded by these genes (Table 4). Therefore, analyzing the potential gene–drug interactions obtained and the category analysis identified for each gene, the drugs for interaction with SLC2A5 (glufosfamide and streptozocin) and with PSMD2 (carfilzomib, bortezomib, ixazomib citrate, and oprozomib) are candidates for in vitro assays (Table 5).

Table 2 Number of differentially expressed genes used to construct interaction networks among SARS-CoV-2-infected cells

GSE access	Cell type	Up	Down
GSE150392	Cardiomyocyte	1404	1543
GSE148729	Caco2	50	33
GSE148729	Calu3	39	21
GSE148729	HT199	2240	1458
GSE153970	Primary human airway epithelial cell (hEC)	463	450
GSE154613	A459 cells expressing human ACE2	204	187
GSE150728	Peripheral blood mononuclear cells	119	70
	Total	4329	3762

Molecular modeling and validation of SLC2A5 and PSMD2 isoforms

The general information for the construction and validation of the three-dimensional models are shown in Table S1. The two SLC2A5 isoforms had excellent qualities, with the MolProbity score being evaluated at the 100th percentile compared to the best three-dimensionally resolved structures. The same can be observed for the three models generated for the PSMD2 isoforms, where the individual percentiles reached were 100, 100, and 99, respectively. The comparison of the models with structures solved using the Z-score and the Ramachandran plot is presented in Fig. S1. All isoforms of SLC2A5 and PSMD2 are distributed within the expected Z-score area (Fig. S1a, c, e, g, i) for proteins of the same size, again providing evidence of the high quality of the models, even for those containing > 900 amino acid residues (PSMD2 isoform 1) (Fig. S1e). Additionally, the SLC2A5 isoform 2 model obtained (Fig. S1c) is compared to the best structures resolved by nuclear magnetic resonance, and the SLC2A5 isoform 1 model (Fig. S1a) stands out for being among the best-resolved structures with the same characteristics. The individual Ramachandran plots are shown in Fig. S1b, d, f, h, and j, where, respectively, 99.4%, 99.6%, 99.8%, 99.6%, and 99.4% are distributed in allowable regions and > 97% of the residues distributed in favorable regions for all models of SLC2A5 and PSMD2, respectively. The superposition of all cured isoforms models can be seen in Fig. S2a.

Molecular docking

The ligands used in the docking simulations (Fig. S2b) had their interaction details with the receptors shown in Table 4. Most of the pockets involved in the ligand–receptor interactions from all structures had promisingly measured druggability scores > 0.8. On the other hand, P7 of isoform 1 and P8 of isoform 2, both from PSMD2, were identified in the interaction interface with carfilzomib.

SLCA2A5

The pocket P0 of SLCA2A5 isoform 1 was responsible for the binding of all docked compounds (Table 5), which represents the open core of the transmembrane channel of the GLUT5 receptor (extracellular face) with a volume of 1899Å^3 (Fig. 3). At P0, the ligand candidates presented the

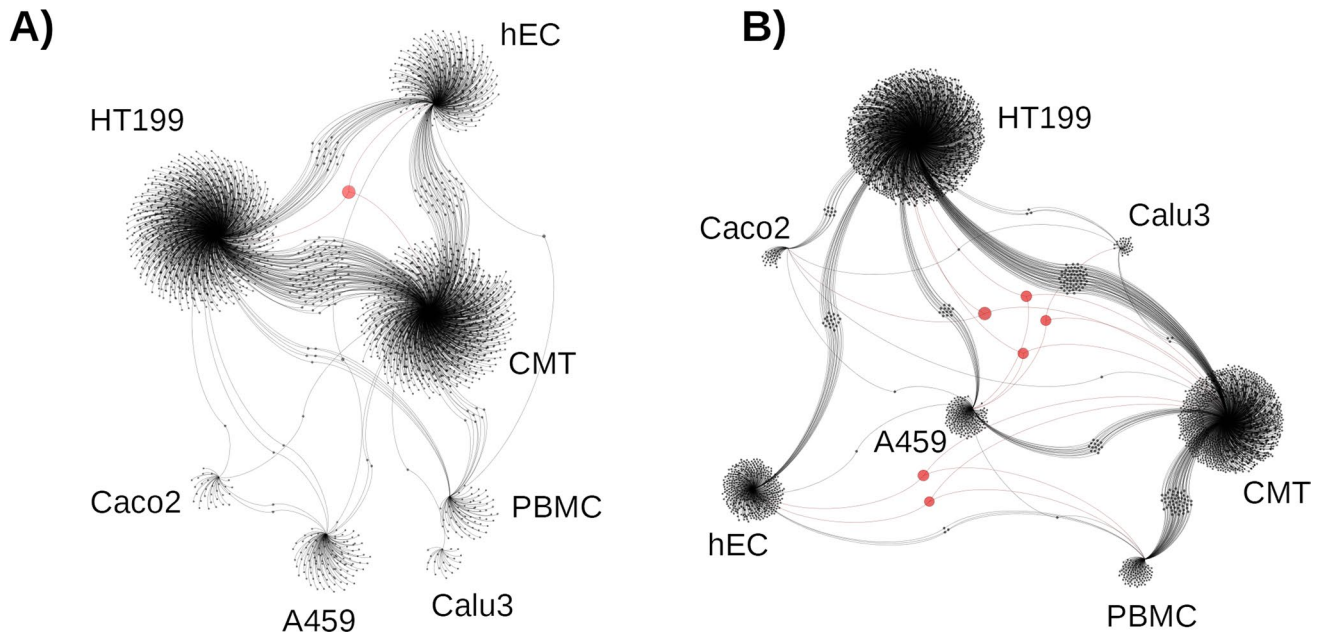

Fig. 2 Network of upregulated and downregulated genes after SARS-COV-2 infection of different human cells types. The bipartite network plot shows a spatially connected network between differentially expressed genes (DEGs) and cell types after SARS-COV-2 infection. Each node represents a gene or cell type. The layout was generated using a force-based algorithm followed by manual rearrangement to visualize the connections better. A total of 8091 DEGs (4329 DEGs with increased expression and 3762 DEGs that had decreased) and seven cell types are represented. Genes shared between three cell types are represented in red. Abbreviations: hEC, human respiratory tract epithelial cells; PBMC, peripheral blood mononuclear cells

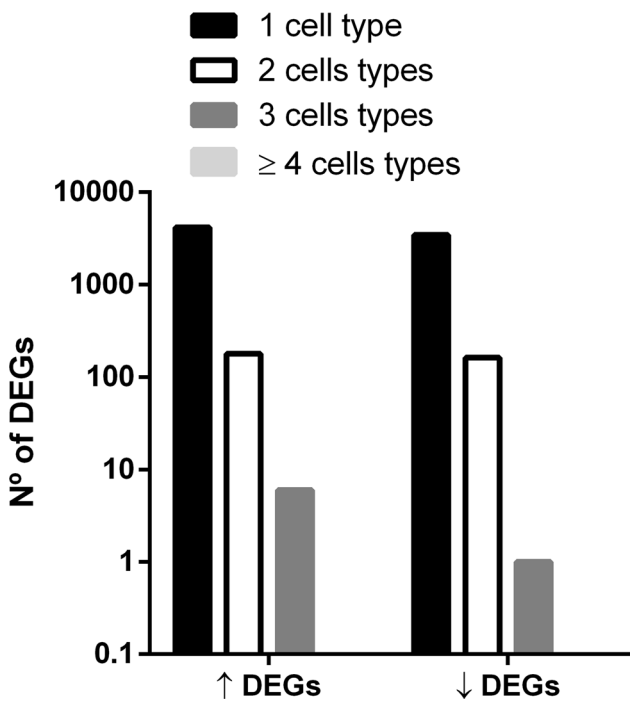

Fig. 3 Number of differentially expressed genes in SARS-COV-2 human-infected cells

same interaction interface when compared to the positive ligand control (D-fructose) and the positive inhibition control (fludeoxyglucose (18F)) (Fig. 3)—indicating potential competitive binding/inhibition property of selected compounds docked in isoform 1. On the other hand, isoform 2 presented distinct interaction pockets (Fig. S3), where the positive controls remained in P0 but at this model with a volume of 1206Å^3. However, the binding candidates were located at P1 (867Å^3), still in the open core of the GLUT5 channel (intracellular face).

Promisingly higher binding energies and higher interface areas (buried surface area (BSA)) ligand–receptor of glufosfamide and streptozocin were observed compared to both binding/inhibition controls (Table 5). In particular, streptozocin presented energy – 6.2 in pocket P0 of isoform1 with BSA of 629Å^2 and – 6.9 in P1 of isoform2 with BSA of 569Å^2. At the observed ligand–receptor interfaces, hydrogen bonds are the main interaction mechanisms presented at the core binding sites of both transmembrane channels (Fig. 4), which is consistent with a large number of hydroxyl groups and amine groups present in the compounds, in addition to an ample supply of acceptors and hydrogen donors in the recipient's residues.

Table 3 List of the genes that were differentially expressed in three cell types after the infection with SARS-COV-2

Gene	Cells type	Expression
IFI44	Cardiomyocyte/human respiratory tract epithelial cells/PBMC	Up
SLC2A5	Cardiomyocyte/human respiratory tract epithelial cells/PBMC	Up
PSMD2	Cardiomyocyte/A549 + hACE2/HT199	Up
PLEKHG6	Cardiomyocyte/A549 + hACE2/HT199	Up
PPP1R15A	Cardiomyocyte/Calu3/A459 + hACE2	Up
CPM	Cardiomyocyte/Caco2/HT199	Up
GNB3	Cardiomyocyte/human respiratory tract epithelial cells/HT199	Down

Table 4 Analysis of potential drugs able to interact with the proteins encoded by the identified genes

		Interaction analysis			
Gene	Category analysis	Drug	Type of interaction	Value	Interaction's value
IFI44	-	U	-	-	-
SLC2A5	Druggable genome transporter	Glufosfamide	U	0.54	3.55
		Streptozocin	U	0.19	1.21
PSMD2	Kinase; clinical action	Carfilzomib	Inhibitory	0.31	1.00
		Bortezomib	Inhibitory	0.29	0.95
		Ixazomib citrate	Inhibitory	0.23	0.75
		Oprozomib	Inhibitory	0.22	0.73
PLEKHG6		U	-	-	-
PPP1R15A		U	-	-	-
CPM	Druggable genome; protease cell surface; enzyme	U	-	-	-
GNB3		Sibutramine	U	1.45	1.45
		Clonidine	U	1.01	1.01
		Torsemide	U	0.73	0.73
		Sildenafil	U	0.67	0.67
		Furosemide	U	0.62	0.62
		Bumetanide	U	0.58	0.58
		Telmisartan	U	0.54	0.55
		Sumatriptan	U	0.48	0.49
		Sertraline	U	0.36	0.36
		Nortriptyline	U	0.36	0.36

U, unidentified

PSMD2

The 3 isoforms of the monomeric 26s proteasome subunits have remarkable structural similarities shown by the overlap (Fig. S2a). However, the binding sites in the receptors were distributed in different ways, with 4, 2, and 1 pockets being observed, respectively (Figs. 5 and S4). Noteworthy is the pocket P3 of isoform 3 with a volume of 983Å^3 and estimated druggability of 0.81 and volume of 2191Å^3. The sharing between the mentioned regions is observed due to the similar interfaces of bortezomib, which is present in P1 of isoforms 1–2, and oprozomib, which is present in P5 of isoform1, partially incorporates the residues of P1 of isoform2 (Figs. 5 and S4)—indicating potential specificity of these compounds to more than one of the monomeric subunit isoforms of the 26 s proteasome. The binding energies varied between − 7.1 and − 8.5 (Table 5), emphasizing the energies and BSA's observed in P3 of isoform 3, slightly higher than in the other isoforms. A great variety of natures of interactions presented by ligand–receptor interaction was observed. In addition to conventional hydrogen bonds, carfilzomib has several pi–alkyl interactions caused by the presence of its two aromatic rings (Figs. 5 and S4).

Table 5 Docking ligand–receptor interaction

	Ligands	Accession (ID)	N° of atoms	Vina score (Kcal/mol)			Pocket (ID & drug score)				Receptor–ligand interface ($Å^2$)			
SLC2A5	Glufosfamide	123,628	43	ISO1	ISO2		ISO1		ISO2		ISO1		ISO2	
	Streptozocin	29,327	33	− 5.8	− 5.7		P0/0.81		P1/0.82		778.3		671.5	
	D-Fructose	37,721	12	− 6.2	− 6.9				P1/0.82		629.4		569.9	
	Fludeoxyglucose (18F)	68,614	13	− 5.6	− 4.9				P0/0.80		490.8		454.2	
				− 5.6	-4.9				P0/0.80		510.7		486.7	
PSMD2	Bortezomib	387,447	53	ISO1	ISO2	ISO3	ISO1	ISO2		ISO3	ISO1	ISO2		ISO3
	Carfilzomib	11,556,711	109	− 7.3	− 7.7	− 7.7	P1/0.8	P1/0.81		P3/0.84	909.4	837.4		1132.3
	Ixazomib Citrate	56,844,015	57	− 7.5	− 8.3	− 8.2	P8/0.45	P7/0.4			1217.6	1478.8		1546.7
	Oprozomib	25,067,547	69	− 7.1	− 7.9	− 8.5	P2/0.82	P0/0.80			908.2	944.3		1148
				− 7.0	− 7.0	− 7.9	P5/0.84	P0/0.80			1082	1064.5		1249.6

Similarly, the influence of bortezomib rings in the presence of pi–cation/anion and pi–alkyl bonds can also be observed, mainly due to the presence of the pyrazine group (Figs. 5 and S4). Furthermore, many hydroxyl groups present in Ixazomib citrate give it a remarkable affinity to the receptor's hydrogen acceptors, with several hydrogen bonds being observed as the primary binding mechanism (Figs. 5 and S4). Finally, oprozomib has, in addition to a large number of hydrogen bonds, the inherent ability to create pi–sulfur interactions due to the existence of sulfur from the thiazole group (Figs. 5 and S4).

Discussion

In late 2019, SARS-CoV-2 emerged in China, and this new coronavirus spread rapidly around the world, configuring itself as one of the most pandemic ever experienced by humankind [6–8]. Due to high transmissibility, the high rate of hospitalization, and death, the development of vaccines and effective antiviral treatment is a priority of many research groups.

Although several studies have identified some effective drugs against SARS-CoV-2, to date, there are few approved effective therapies for COVID-19. Most of them are monoclonal antibodies (e.g., regdanvimab, tocilizumab, sotrovimab, and casirivimab/imdevimab), but there is also one antiviral drug (remdesivir) [49]. Therefore, there is an urgent need to identify new viral and cellular targets that could be useful to identify new antiviral compounds or be useful for repurposing drugs.

In this study, we used an in silico protocol to integrate different transcriptome data combined with deep learning algorithms to identify candidate genes important to the development of antiviral treatment of COVID-19. By this approach, it was verified that there is a specific transcriptional response of cells to SARS-CoV-2 infection since few DEGS are shared between the cells (Figs. 2 and 3). This specific transcriptional response for each cell type can also reflect the different times of infection, which ranged from 24 to 72 h, in an asynchrony condition (started with MOI < 0.3) (Table 1). Consequently, most cells of each cell model analyzed could be at different times of the replication cycle and justify the different expression patterns between these cell models. After all, the replication kinetics of SARS-CoV-2 is influenced by the host cell, and the virus's modulation of host gene expression will also depend on the replication and transcription step of SARS-CoV-2 itself in that cell [50–53], and this could explain why few DEGS are shared between the cell types. ITA was able to identify some potential targets for the treatment of coronavirus disease (Table 3), with some of the potential to be a target for the development of new treatment strategies for COVID-19 (Table 4).

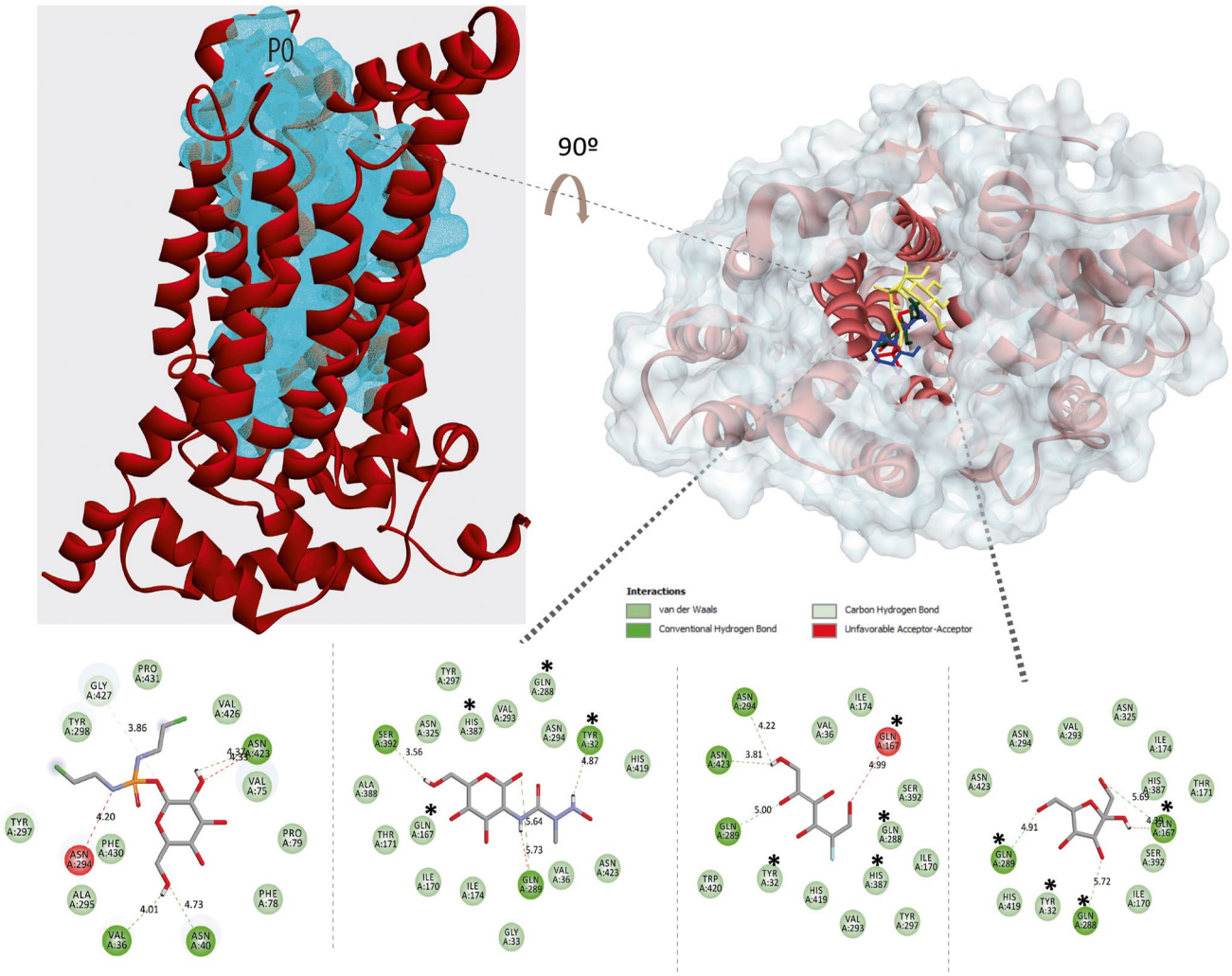

Fig. 4 SLC25A binding site isoform 1. Isoform 1 was represented as cartoons on the top left with their respective surface binding pockets. Isoform 1 in the cartoon with a transparent surface on the right, showing the open channel with all the ligands in pocket P0. At the bottom, the 2D maps of the interactions are represented, containing from left to right: glufosfamide, streptozocin, fludeoxyglucose (18F), and D-fructose are represented in stick, with all the amino acid residues involved in the interaction described by balloons. The hydrogen donor/acceptor interactions are characterized by a dotted line with their respective distances. Shaded areas on atoms from balloons indicate solvent exposure. The asterisk points out the key residues binding to the natural substrate (D-fructose)

Among these DEGs, two upregulated DEGs encoded proteins that can be used as antiviral targets. The SLC2A5 gene encodes a fructose transporter responsible for fructose uptake and therefore for energetic metabolism [54, 55]. The PDSM2 gene encodes a component of the 26S proteasome, a multiprotein complex involved in the ATP-dependent degradation of ubiquitinated proteins [56]. These two proteins have recently attracted attention for their druggable and therapeutic potential [57, 58].

Our analysis identified SLC2A5 as an upregulated DEG in three SARS-CoV-2 infected cells (cardiomyocyte, human respiratory tract epithelial cells, and PBMC). The SLC2A5 gene was reported as one of many genes differentially expressed related to a severe neurological progression in COVID-19 patients [59]. It also demonstrated high levels of fructose in PBMC [60] and serum metabolome of SARS-CoV-2 patients [61]. The high levels of this metabolite can also induce glycolysis in SARS-CoV-2-infected human monocytes [62]. These data suggest an increasing need for energy production in SARS-CoV-2-infected cells since fructose could be an efficient carbon and energy source. Therefore, higher levels of fructose would require greater transport efficiency into the cell, which could explain the higher expression of the SLC2A5 gene to supply the energy needs of the infected cells.

Other viruses are known to manipulate other glucose transporters to increase the acquisition of their target carbohydrate. For example, the human immunodeficiency virus led

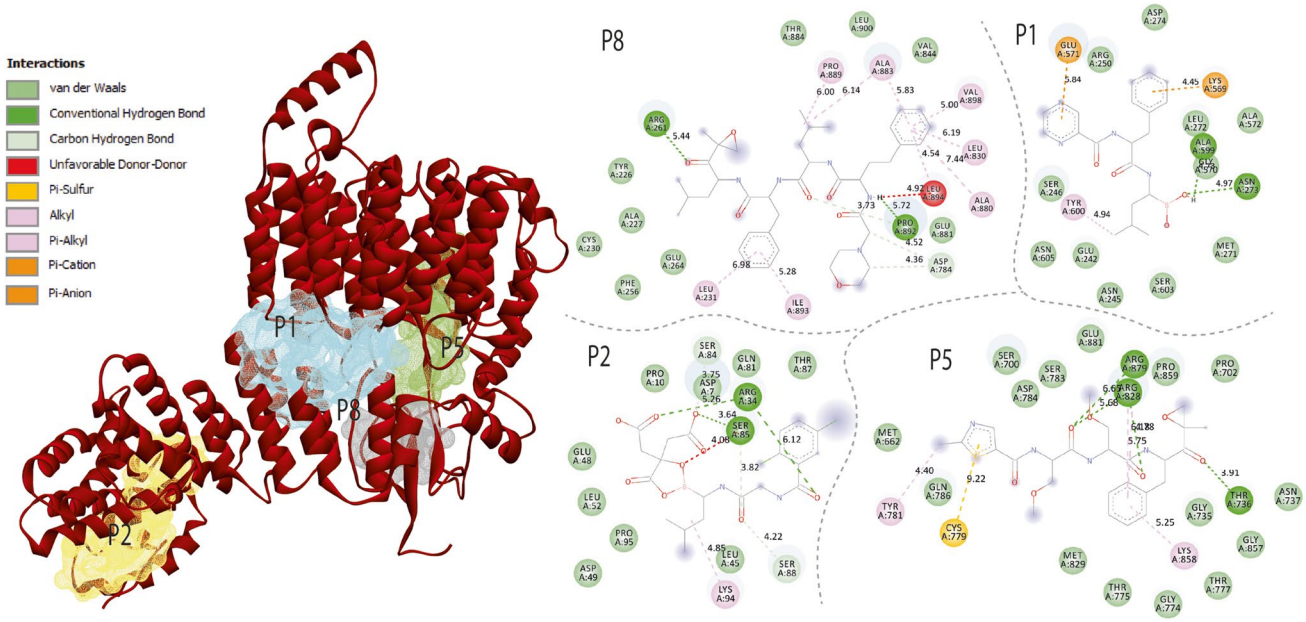

Fig. 5 PSMD2 binding site isoform 1. On the left, isoform 1 was represented as cartoons with their respective surface binding pockets. On the right, the ligands are represented in 2D interaction maps. The first pair of ligands is represented by lines, from left to right: carfilzomib and bortezomib and, the second pair, ixazomib and oprozomib. Balloons represent the amino acid residues involved in the interaction. The hydrogen donor/acceptor interactions, pi–sulfur, pi–cation, and pi–anion are characterized by a dotted line with their respective distances. Shaded areas on atoms and balloons indicate solvent exposure

to an increased expression of GLUT3 and increased glucose transport in H9 lymphocytic infected cells [63]. In addition, the human cytomegalovirus replaces GLUT1 with GLUT4, abundant in adipose tissue, and increases glucose transport capacity [64]. In this particular case, this change in GLUTs appears essential in cytomegalovirus infection of fibroblasts; once the function is specifically inhibited, the result is not only less glucose uptake but also dramatically inhibits the formation of infectious viral infection progeny [64, 65].

Therefore, an increase of the expression of SLC2A5 in SARS-CoV-2-infected cells derived from heart and lung tissues could be important to the pathophysiology of COVID-19 once these organs are two important systems affected COVID-19 patients. It is also suggested that the increase in glycolysis induced by SARS-CoV-2 infection may also be an important factor in cytokine regulation [62]. An increased expression of SLC2A5 by SARS-CoV-2 may represent a vital mechanism of infection, and inhibiting it could lead to a significant reduction in viral production. Previously, the inhibition of glycolysis by 2-deoxy-D-glucose prevents conversion to fructose, and this event resulted in inhibition of SARS-CoV-2 replication in a colon adenocarcinoma cell (Caco-2) line and monocytes [62, 66, 67].

Once it was understood that the SLC2A5 is a potential target for the control of SARS-CoV-2 replication, this enzyme was modeled to be later used to search for potential inhibitors of the target and, consequently, viral replication. The molecular modeling of GLUT-5 included the three-dimensional models of its isoforms (Table S1) derived from the alternative-splicing demonstrated in accessions P22732 and Q13200 (Uniprot ID). Even though interactions with the lipid bilayer make it particularly difficult to achieve high-quality resolution of transmembrane transporters [68], the complete structure of GLUT-5 presented here offers quality comparable to the best structures ever solved in PDB (Fig. S1), providing a unique path to search for potential drugs from its three-dimensional model.

The molecular modeling allowed determining the druggable regions classified in different pockets and starting the search for putative ligands. D-Fructose was used as an empirical reference of potential new ligands. Fludeoxyglucose (18F), an experimentally known inhibitor of the sugar transport function [69], was also included in the analysis. It was also considered the "open core of the channel," which has the hotspot binding points characterized for the amino acid residues 32TYR, 167GLN, 288GLN, and 387HIS responsible for the binding site of the transmembrane receptor SLC2A5 to D-fructose [70]. All these benchmarks were considered for the new putative ligand/inhibitor appointment.

The accuracy of the receptor–ligand binding is supported by the result of the docking simulation with D-fructose which presented an interaction interface with its respective natural binding site, constituting interactions with all

key residues and observed for the fludeoxyglucose (18F) (Fig. 3). Furthermore, both molecules were observed in pocket P1 with the same − 5.6 kcal/mol of Vina score and with a high similar BSA score (Table 4). These data suggest that a competitive inhibition mechanism of SLC2A5 in this region could be important to find new potential drugs for inhibiting SLC2A5 activity.

Through the binding and inhibition references presented, we promisingly point to the putative inhibition of SLC2A5 by streptozocin through comparison with the fludeoxyglucose (18F) binding site in pocket P1. Streptozocin presents a binding interface with all the key residues observed in Fig. 3. Additionally, streptozocin had a higher Vina (− 6.2 kcal/mol) and BSA (629.4 $Å^2$) score than the known inhibitor, making it a candidate for inhibiting sugar transport also through competition. Streptozocin is particularly an eclectic drug; it was first discovered as an antibiotic against Gram-negative bacteria once it inhibits the synthesis of DNA in microorganisms and mammalian cells [71, 72]. It is also used as a chemotherapeutic drug for treating certain pancreatic cancers and was approved to be used in the USA in 1982. The anticancer activity is due to the inhibition of glucose transporter 2 (GLUT2) expressed at pancreatic beta cells [71, 73]. These data strengthen the potential of streptozocin to be used in in vitro and in vivo assays, and therefore, new experiments should be performed to determine if the inhibition of GLUT-5 activity could reduce viral replication.

Our analysis also indicates that the ubiquitin–proteasome system is a potential target to develop antivirals against SARS-CoV-2. This intracellular system has a crucial role in the degradation of most cellular proteins, including short-lived, regulatory, and misfolded/denatured proteins [74, 75]. While viruses evolved, exploiting the cellular machinery and taking control of a protein degradation system are undoubtedly an adaptive advantage. Therefore, it is not surprising that viruses induce proteasome regulation after cellular infection. The proteasome can play an antiviral role in response to many infections, through degradation of viral proteins (e.g., West Nile virus and hepatitis C virus) or suppressing viral protein activity by ISGylation (e.g., influenza A virus and human papillomavirus) [76–78], although many other pro-viral functions are reported [79].

Viruses such as adenovirus and human immunodeficiency viruses 1 and 2 use proteasome to regulate cellular protein degradation [80, 81]. However, others may employ this system to maintain proper levels of viral proteins (e.g., human papillomavirus and hepatitis C virus) [82, 83]. It was described that SARS-CoV might use the proteasome for its benefit, counteracting the post-translational modification of signaling molecules involved in innate immunity. The papain-like protease of SARS-CoV can promote deubiquitinating (and deISGylating) that are proposed to counteract the post-translational modification of signaling molecules that activate the innate immune response [79, 84]. At least two other SARS-CoV proteins interact with this system. The E protein interacts with the non-structural protein 3 to be ubiquitinated and the N protein with the host cell proteasome subunit p42, a 26S proteasome subunit [85, 86].

Since the proteasome system plays an important role during the SARS-CoV infection cycle, proteasome inhibition appears to be a promising strategy in combating SARS-CoV-2 infection. Proteasome inhibition leads to the accumulation of polyubiquitinated proteins in the cytoplasm [87]. This unbalanced protein homeostasis leads to a cellular stress response that can be responsible for the induction of cell death [87, 88].

The inhibition of the proteasome with different compounds, such as MG132 and epoxomicin, leads to impaired viral entry and a decrease of RNA synthesis and protein expression of different coronaviruses [89]. On the other hand, a study demonstrated that the inhibition of SARS-CoV replication by MG132 occurs independently of inhibition of the proteasome system [90]. Although this potential of proteasome inhibitors has been suggested to combat SARS-CoV-2 infection, we do not know that they have been used in clinical trials.

Notwithstanding, a proteasome inhibitor (α-keto phenylamide) derivative compound demonstrated an anti-SARS-CoV-2 activity. However, the authors associated the viral progeny reduction with an interaction with the virus's protease [91]. Anyway, it seems plausible to consider proteasome inhibitors as a target for the search for drugs that inhibit viral replication, especially if we consider the expression profile of the proteasome observed by our integrative analysis and its roles in the control of coronaviruses replication.

Large polypeptide chains are difficult to model without high-quality homologous templates. The three-dimensional structures of the 26 s proteasome subunits are known from the 6MSK crystal (PDB ID). However, dozens of monomers are incomplete and mostly resolved at low resolutions. Therefore, it was relevant to obtain high-quality three-dimensional models for the monomeric chain of the 26S proteasome (Fig. S1e and S1j) before starting the search for its putative inhibitors.

The 26 s proteasome showed four high druggability different pockets of ligand–receptor interaction, each containing distinct and promising interaction profiles (Fig. 4). Besides, recent studies reported curcumin, LDN192960, and oprozomib as 26 s proteasome inhibitors, the pathways responsible for its inhibition are poorly understood. Therefore, there are no specific ligands/inhibitors that can be used as controls in docking studies using the 26 s proteasome [92–94].

Nevertheless, four ligands have been identified, and they had similar binding energy scores (from − 7.0 to − 7.5). The compound ixazomib citrate is promisingly docked to P2 in the N-terminal portion of the 26 s proteasome (Fig. 4). The N-terminal portion is understood as an attractive drug target once it constitutes a regulatory region of the 26 s proteasome [95]. The ligands bortezomib and oprozomib interact in P1 and P5, respectively. These two regions are both considered promising druggable pockets (Table 4) located around the dozens of helices in the structural center of the monomer. On the other hand, carfilzomib has the largest binding interface area and Vina energy score (Table 4). However, it is located at P8, with a low estimated druggability (0.45).

These compounds are already known as proteasome inhibitors and are used/suggested for anti-myeloma therapy [96]. Bortezomib reversibly binds with high affinity to the 26S proteasome β-subunit [97]. This drug has been recommended in treating adult patients with multiple myeloma cell lymphoma by the Food and Drug Administration (FDA) since 2003 [98]. Ixazomib binds and inhibits the β5 subunit of the 20S proteasome and has been approved by the FDA in 2015 for use in the treatment of patients with multiple myeloma [99]. Unlike bortezomib, the carfilzomib, approved in 2012 by the FDA, binds irreversibly and selectively to the chymotrypsin-like activity region of the 20S proteasome [100, 101]. Oprozomib is a second-generation proteasome inhibitor, which the US FDA has also approved for clinical treatment of recurrent multiple myeloma [102, 103].

Identifying new uses outside the original indication for approved or investigational drugs has become a very desired strategy, especially with the need to treat COVID-19 [104–106]. This strategy, known as drug repurposing, offers various advantages over developing an entirely new drug. For example, drug repurposing has a lower failure risk and reduced drug development and approval [105, 107]. In this study, we used several bioinformatic tools to find new drugs that could repurpose drugs for different COVID-19. Through the initial integrative analysis, genes that are differentially expressed during the infection in cells from different tissues are determined, resulting in an almost global pattern of infection. This previously determined pattern will guide the subsequent modeling of the targets selected by this integrative transcriptomic analysis of machine learning structural modeling. Furthermore, molecular docking would allow identifying available drugs that interact with the targets and propose laboratory and clinical essays for proof of concept. This represents a bioinformatics tool for screening molecules tested for new uses, saving financial resources time, and making a personalized screening for each infectious disease.

Supplementary information The online version contains supplementary material available at https://doi.org/10.1007/s42770-022-00875-2.

Acknowledgements A special acknowledgement to Renato Fróes Goulart de Castro (in memoriam) for all his time working with us, for his dedication and friendship. We regret that he could not have seen more of this published work.

Author contribution All authors contributed to the study's conception and design. Material preparation, data collection, and analysis were performed by Ricardo Lemes Gonçalves, Gabriel Augusto Pires de Souza, Renato Fróes Goulart de Castro, and Luiz Felipe Leomil Coelho. The first draft of the manuscript was written by Ricardo Lemes Gonçalves, Gabriel Augusto Pires de Souza, and Luiz Felipe Leomil Coelho. All authors commented on previous versions of the manuscript. Finally, all authors read and approved the final manuscript.

Funding This work was funded by the Fundação de Amparo a Pesquisa do Estado de Minas Gerais (FAPEMIG) (grants number APQ-01165–16 and PPM-00399–18); the Coordenacao de Aperfeicoamento de Pessoal de Nivel Superior, Brazil (CAPES) (Finance Code 001); and the Conselho Nacional de Desenvolvimento Científico e Tecnológico (CNPq).

Availability of data and material Not applicable.

Code availability Not applicable.

Declarations

Consent to participate Not applicable.

Consent for publication Not applicable.

Conflict of interest The authors declare no competing interests.

References

1. Cui J, Li F, Shi ZL (2019) Origin and evolution of pathogenic coronaviruses. Nat Rev Microbiol 17:181–192. https://doi.org/10.1038/s41579-018-0118-9
2. Hu B, Guo H, Zhou P (2020) Shi ZL (2020) Characteristics of SARS-CoV-2 and COVID-19. Nat Rev Microbiol 193(19):141–154. https://doi.org/10.1038/S41579-020-00459-7
3. Zhong NS, Zheng BJ, Li YM et al (2003) Epidemiology and cause of severe acute respiratory syndrome (SARS) in Guangdong, People's Republic of China, in February, 2003. Lancet (London, England) 362:1353–1358. https://doi.org/10.1016/S0140-6736(03)14630-2
4. Zaki AM, van Boheemen S, Bestebroer TM et al (2012) Isolation of a novel coronavirus from a man with pneumonia in Saudi Arabia. N Engl J Med 367:1814–1820. https://doi.org/10.1056/NEJMOA1211721
5. van Boheemen S, de Graaf M, Lauber C et al (2012) Genomic characterization of a newly discovered coronavirus associated with acute respiratory distress syndrome in humans. MBio 3(6):e473–12. https://doi.org/10.1128/MBIO.00473-12
6. Wu F, Zhao S, Yu B et al (2020) A new coronavirus associated with human respiratory disease in China. Nat 5797798(579):265–269. https://doi.org/10.1038/S41586-020-2008-3
7. Hui DS, I Azhar E, Madani TA et al (2020) The continuing 2019-nCoV epidemic threat of novel coronaviruses to global health — the latest 2019 novel coronavirus outbreak in Wuhan, China. Int J Infect Dis 91:264–266.https://doi.org/10.1016/j.ijid.2020.01.009

8. WHO (2020) Coronavirus disease 2019 (COVID-19): situation report, 61. https://apps.who.int/iris/handle/10665/331605. Accessed 24 Jan 2022
9. Lu R, Zhao X, Li J et al (2020) Genomic characterisation and epidemiology of 2019 novel coronavirus: implications for virus origins and receptor binding. Lancet 395:565–574. https://doi.org/10.1016/S0140-6736(20)30251-8/ATTACHMENT/1686D69B-3F2C-44B2-A8A5-C648EF9D1C2B/MMC1.PDF
10. Chan JFW, Yuan S, Kok KH et al (2020) A familial cluster of pneumonia associated with the 2019 novel coronavirus indicating person-to-person transmission: a study of a family cluster. Lancet 395:514–523. https://doi.org/10.1016/S0140-6736(20)30154-9
11. Deng SQ, Peng HJ (2020) Characteristics of and public health responses to the coronavirus disease 2019 outbreak in China. J Clin Med 9(2):575. https://doi.org/10.3390/JCM9020575
12. Chen R, Liang W, Jiang M et al (2020) Risk factors of fatal outcome in hospitalized subjects with coronavirus disease 2019 from a nationwide analysis in China. Chest 158:97–105. https://doi.org/10.1016/j.chest.2020.04.010
13. Han Q, Lin Q, Jin S, You L (2020) Coronavirus 2019-nCoV: a brief perspective from the front line. J Infect 80:373–377. https://doi.org/10.1016/J.JINF.2020.02.010
14. Li Y, Xie Z, Lin W et al (2020) Efficacy and safety of lopinavir/ritonavir or Arbidol in adult patients with mild/moderate COVID-19: an exploratory randomized controlled trial. Med (New York, NY) 1:105-113.e4. https://doi.org/10.1016/J.MEDJ.2020.04.001
15. Lian N, Xie H, Lin S et al (2020) Umifenovir treatment is not associated with improved outcomes in patients with coronavirus disease 2019: a retrospective study. Clin Microbiol Infect 26:917–921. https://doi.org/10.1016/J.CMI.2020.04.026
16. Wang M, Cao R, Zhang L et al (2020) Remdesivir and chloroquine effectively inhibit the recently emerged novel coronavirus (2019-nCoV) in vitro. Cell Res 30:269–271. https://doi.org/10.1038/S41422-020-0282-0
17. Rosenberg ES, Dufort EM, Udo T et al (2020) Association of treatment with hydroxychloroquine or azithromycin with in-hospital mortality in patients with COVID-19 in New York state. JAMA 323:2493–2502. https://doi.org/10.1001/JAMA.2020.8630
18. Monteil V, Kwon H, Prado P et al (2020) Inhibition of SARS-CoV-2 infections in engineered human tissues using clinical-grade soluble human ACE2. Cell 181:905-913.e7. https://doi.org/10.1016/j.cell.2020.04.004
19. Tian X, Li C, Huang A et al (2020) Potent binding of 2019 novel coronavirus spike protein by a SARS coronavirus-specific human monoclonal antibody. Emerg Microbes Infect 9:382–385. https://doi.org/10.1080/22221751.2020.1729069
20. Tahir ul Qamar M, Alqahtani SM, Alamri MA, Chen LL (2020) Structural basis of SARS-CoV-2 3CL pro and anti-COVID-19 drug discovery from medicinal plants. J Pharm Anal 10:313–319.https://doi.org/10.1016/J.JPHA.2020.03.009
21. Williamson BN, Feldmann F, Schwarz B et al (2020) (2020) Clinical benefit of remdesivir in rhesus macaques infected with SARS-CoV-2. Nat 5857824(585):273–276. https://doi.org/10.1038/S41586-020-2423-5
22. Cai Q, Yang M, Liu D et al (2020) Experimental treatment with favipiravir for COVID-19: an open-label control study. Eng (Beijing, China) 6:1192–1198. https://doi.org/10.1016/J.ENG.2020.03.007
23. Cao B, Wang Y, Wen D et al (2020) A trial of lopinavir–ritonavir in adults hospitalized with severe Covid-19. N Engl J Med 382:1787–1799. https://doi.org/10.1056/NEJMOA2001282/SUPPL_FILE/NEJMOA2001282_DATA-SHARING.PDF
24. Hung IFN, Lung KC, Tso EYK et al (2020) Triple combination of interferon beta-1b, lopinavir–ritonavir, and ribavirin in the treatment of patients admitted to hospital with COVID-19: an open-label, randomised, phase 2 trial. Lancet 395:1695–1704. https://doi.org/10.1016/S0140-6736(20)31042-4/ATTACHMENT/4753030C-5333-4ABE-BE66-F099C5E96D3A/MMC1.PDF
25. Xu X, Han M, Li T et al (2020) Effective treatment of severe COVID-19 patients with tocilizumab. Proc Natl Acad Sci U S A 117:10970–10975. https://doi.org/10.1073/PNAS.2005615117
26. Diurno F, Numis FG, Porta G et al (2020) Eculizumab treatment in patients with COVID-19: preliminary results from real life ASL Napoli 2 Nord experience. Eur Rev Med Pharmacol Sci 24:4040–4047. https://doi.org/10.26355/EURREV_202004_20875
27. Duan K, Liu B, Li C et al (2020) Effectiveness of convalescent plasma therapy in severe COVID-19 patients. Proc Natl Acad Sci U S A 117:9490–9496. https://doi.org/10.1073/PNAS.2004168117
28. Zost SJ, Gilchuk P, Case JB et al (2020) (2020) Potently neutralizing and protective human antibodies against SARS-CoV-2. Nat 5847821(584):443–449. https://doi.org/10.1038/S41586-020-2548-6
29. Park A, Iwasaki A (2020) Type I and type III interferons - induction, signaling, evasion, and application to combat COVID-19. Cell Host Microbe 27:870–878. https://doi.org/10.1016/J.CHOM.2020.05.008
30. Shen C, Wang Z, Zhao F et al (2020) Treatment of 5 critically Ill patients with COVID-19 with convalescent plasma. JAMA 323:1582–1589. https://doi.org/10.1001/JAMA.2020.4783
31. Berkhout B, Coombs KM (2013) Quantitative omics and its application to study virus-host interactions-a new frontier. Front Microbiol 4:31. https://doi.org/10.3389/FMICB.2013.00031/BIBTEX
32. Jean Beltran PM, Federspiel JD, Sheng X, Cristea IM (2017) Proteomics and integrative omic approaches for understanding host–pathogen interactions and infectious diseases. Mol Syst Biol 13(3):922. https://doi.org/10.15252/MSB.20167062
33. Tulsyan S, Hussain S, Mittal B et al (2020) A systematic review with in silico analysis on transcriptomic profile of gallbladder carcinoma. Semin Oncol 47:398–408. https://doi.org/10.1053/J.SEMINONCOL.2020.02.012
34. Pires de Souza GA, Salvador EA, de Oliveira FR et al (2020) An in silico integrative protocol for identifying key genes and pathways useful to understand emerging virus disease pathogenesis. Virus Res 284:197986. https://doi.org/10.1016/j.virusres.2020.197986
35. Cinegaglia NC, Andrade SCS, Tokar T et al (2016) Integrative transcriptome analysis identifies deregulated microRNA-transcription factor networks in lung adenocarcinoma. Oncotarget 7:28920–28934. https://doi.org/10.18632/ONCOTARGET.8713
36. Hoshida Y, Nijman SMB, Kobayashi M et al (2009) Integrative transcriptome analysis reveals common molecular subclasses of human hepatocellular carcinoma. Cancer Res 69:7385–7392. https://doi.org/10.1158/0008-5472.CAN-09-1089
37. Liao Q, Wang J, Pei Z et al (2017) Identification of miRNA-mRNA crosstalk in CD4+ T cells during HIV-1 infection by integrating transcriptome analyses. J Transl Med 15:1–11. https://doi.org/10.1186/S12967-017-1130-Y/FIGURES/2
38. Moslehi R, Mills JL, Signore C et al (2013) (2013) Integrative transcriptome analysis reveals dysregulation of canonical cancer molecular pathways in placenta leading to preeclampsia. Sci Reports 31(3):1–11. https://doi.org/10.1038/SREP02407
39. Raj T, Li YI, Wong G et al (2018) (2018) Integrative transcriptome analyses of the aging brain implicate altered splicing in Alzheimer's disease susceptibility. Nat Genet 5011(50):1584–1592. https://doi.org/10.1038/S41588-018-0238-1

40. Vavougios GD, Nday C, Pelidou SH et al (2020) Double hit viral parasitism, polymicrobial CNS residency and perturbed proteostasis in Alzheimer's disease: a data driven, in silico analysis of gene expression data. Mol Immunol 127:124–135. https://doi.org/10.1016/J.MOLIMM.2020.08.021
41. Bastian M, Heymann S, Jacomy M (2009) Gephi: an open source software for exploring and manipulating networks. Proc Int AAAI Conf Web Soc Media 3(1):361–362. https://doi.org/10.1609/ICWSM.V3I1.13937
42. Jumper J, Evans R, Pritzel A et al (2021) (2021) Highly accurate protein structure prediction with AlphaFold. Nat 5967873(596):583–589. https://doi.org/10.1038/S41586-021-03819-2
43. Baek M, DiMaio F, Anishchenko I et al (2021) Accurate prediction of protein structures and interactions using a three-track neural network. Science (80)373:871–876. https://doi.org/10.1126/science.abj8754
44. Williams CJ, Headd JJ, Moriarty NW et al (2018) MolProbity: more and better reference data for improved all-atom structure validation. Protein Sci 27:293–315. https://doi.org/10.1002/PRO.3330
45. Heo L, Lee H, Seok C (2016) GalaxyRefineComplex: refinement of protein-protein complex model structures driven by interface repacking. Sci Reports 6(1):1–10. https://doi.org/10.1038/srep32153
46. Wiederstein M, Sippl MJ (2007) ProSA-web: interactive web service for the recognition of errors in three-dimensional structures of proteins. Nucleic Acids Res 35:W407–W410. https://doi.org/10.1093/NAR/GKM290
47. Trott O, Olson AJ (2010) AutoDock Vina: improving the speed and accuracy of docking with a new scoring function, efficient optimization and multithreading. J Comput Chem 31:455. https://doi.org/10.1002/JCC.21334
48. Yuan S, Chan HCS, Hu Z (2017) Using PyMOL as a platform for computational drug design. Wiley Interdiscip Rev Comput Mol Sci 7:e1298. https://doi.org/10.1002/WCMS.1298
49. European Medicines Agency (2021) COVID-19 treatments: authorised. https://www.ema.europa.eu/en/human-regulatory/overview/public-health-threats/coronavirus-disease-covid-19/treatments-vaccines/treatments-covid-19/covid-19-treatments-authorised. Accessed 24 Dec 2021
50. Malone B, Urakova N, Snijder EJ, Campbell EA (2022) Structures and functions of coronavirus replication–transcription complexes and their relevance for SARS-CoV-2 drug design. Nat Rev Mol Cell Biol 23:21–39. https://doi.org/10.1038/s41580-021-00432-z
51. Mautner L, Hoyos M, Dangel A et al (2022) Replication kinetics and infectivity of SARS-CoV-2 variants of concern in common cell culture models. Virol J 19:1–11. https://doi.org/10.1186/s12985-022-01802-5
52. V'kovski P, Kratzel A, Steiner S et al (2021) Coronavirus biology and replication: implications for SARS-CoV-2. Nat Rev Microbiol 19:155–170. https://doi.org/10.1038/s41579-020-00468-6
53. Pires De Souza GA, Le Bideau M, Boschi C et al (2022) Choosing a cellular model to study SARS-CoV-2. Front Cell Infect Microbiol 12:1583. https://doi.org/10.3389/FCIMB.2022.1003608/BIBTEX
54. Kayano T, Burant CF, Fukumoto H et al (1990) Human facilitative glucose transporters. Isolation, functional characterization, and gene localization of cDNAs encoding an isoform (GLUT5) expressed in small intestine, kidney, muscle, and adipose tissue and an unusual glucose transporter pseudogene-like. J Biol Chem 265:13276–13282. https://doi.org/10.1016/s0021-9258(19)38295-x
55. Zwarts I, van Zutphen T, Kruit JK et al (2019) Identification of the fructose transporter GLUT5 (SLC2A5) as a novel target of nuclear receptor LXR. Sci Rep 9:1–10. https://doi.org/10.1038/s41598-019-45803-x
56. Kanayama H-o, Tamura T, Ugai S et al (1992) Demonstration that a human 26S proteolytic complex consists of a proteasome and multiple associated protein components and hydrolyzes ATP and ubiquitin-ligated proteins by closely linked mechanisms. Eur J Biochem 206:567–578. https://doi.org/10.1111/j.1432-1033.1992.tb16961.x
57. Longhitano L, Tibullo D, Giallongo C et al (2020) Proteasome inhibitors as a possible therapy for SARS-CoV-2. Int J Mol Sci 21:1–11. https://doi.org/10.3390/ijms21103622
58. Ferreira RS, Pons JL, Labesse G (2019) Insights into substrate and inhibitor selectivity among human GLUT transporters through comparative modeling and molecular docking. ACS Omega 4:4748–4760. https://doi.org/10.1021/ACSOMEGA.8B03447
59. Rahman MH, Rana HK, Peng S et al (2021) Bioinformatics and system biology approaches to identify pathophysiological impact of COVID-19 to the progression and severity of neurological diseases. Comput Biol Med 138:104859. https://doi.org/10.1016/J.COMPBIOMED.2021.104859
60. Singh Y, Trautwein C, Fendel R et al (2021) SARS-CoV-2 infection paralyzes cytotoxic and metabolic functions of the immune cells. Heliyon 7:e07147. https://doi.org/10.1016/J.HELIYON.2021.E07147
61. Shi D, Yan R, Lv L et al (2021) The serum metabolome of COVID-19 patients is distinctive and predictive. Metabolism 118:154739. https://doi.org/10.1016/J.METABOL.2021.154739
62. Codo AC, Davanzo GG, de Brito Monteiro L et al (2020) Elevated glucose levels favor SARS-CoV-2 infection and monocyte response through a HIF-1α/glycolysis-dependent axis. Cell Metab 32(3):437–446.e5. https://doi.org/10.1016/j.cmet.2020.07.007
63. Sorbara LR, Maldarelli F, Chamoun G et al (1996) Human immunodeficiency virus type 1 infection of H9 cells induces increased glucose transporter expression. J Virol 70:7275–7279. https://doi.org/10.1128/jvi.70.10.7275-7279.1996
64. Yu Y, Maguire TG, Alwine JC (2011) Human cytomegalovirus activates glucose transporter 4 expression to increase glucose uptake during infection. J Virol 85:1573–1580. https://doi.org/10.1128/jvi.01967-10
65. Yu Y, Clippinger AJ, Alwine JC (2011) Viral effects on metabolism: changes in glucose and glutamine utilization during human cytomegalovirus infection. Trends Microbiol 19:360–367. https://doi.org/10.1016/j.tim.2011.04.002
66. Bojkova D, Klann K, Koch B et al (2020) Proteomics of SARS-CoV-2-infected host cells reveals therapy targets. Nature 583:469–472. https://doi.org/10.1038/s41586-020-2332-7
67. Bojkova D, Costa R, Reus P et al (2021) Targeting the pentose phosphate pathway for SARS-CoV-2 therapy. Metab. https://doi.org/10.3390/metabo11100699
68. Kermani AA, Kermani AA (2021) A guide to membrane protein X-ray crystallography. FEBS J 288:5788–5804. https://doi.org/10.1111/FEBS.15676

69. Trayner BJ, Grant TN, West FG, Cheeseman CI (2009) Synthesis and characterization of 6-deoxy-6-fluoro-d-fructose as a potential compound for imaging breast cancer with PET. Bioorganic Med Chem 17:5488–5495. https://doi.org/10.1016/j.bmc.2009.06.034
70. Nomura N, Verdon G, Kang HJ et al (2015) Structure and mechanism of the mammalian fructose transporter GLUT5. Nature 526:397. https://doi.org/10.1038/NATURE14909
71. Abdollahi M, Hosseini A (2014) Streptozotocin. Encycl Toxicol (3rd edn.) 402–404. https://doi.org/10.1016/B978-0-12-386454-3.01170-2
72. Aoki T, Kokudo N, Komoto I et al (2015) Streptozocin chemotherapy for advanced/metastatic well-differentiated neuroendocrine tumors: an analysis of a multi-center survey in Japan. J Gastroenterol 50:769–775. https://doi.org/10.1007/s00535-014-1006-3
73. Rosati M (2017) Saunders handbook of veterinary drugs: small and large animals, 4th edn. Can Vet J 58(7):728. https://doi.org/10.1016/B978-0-323-70957-6.01001-3
74. Gong B, Radulovic M, Figueiredo-Pereira ME, Cardozo C (2016) The ubiquitin-proteasome system: potential therapeutic targets for Alzheimer's disease and spinal cord injury. Front Mol Neurosci 9:1–16. https://doi.org/10.3389/fnmol.2016.00004
75. Schwartz AL, Ciechanover A (2009) Targeting proteins for destruction by the ubiquitin system: implications for human pathobiology. Annu Rev Pharmacol Toxicol 49:73–96. https://doi.org/10.1146/annurev.pharmtox.051208.165340
76. Durfee LA, Lyon N, Seo K, Huibregtse JM (2010) The ISG15 conjugation system broadly targets newly synthesized proteins: implications for the antiviral function of ISG15. Mol Cell 38:722–732. https://doi.org/10.1016/j.molcel.2010.05.002
77. Ko A, Lee E-W, Yeh J-Y et al (2010) MKRN1 induces degradation of west nile virus capsid protein by functioning as an E3 ligase. J Virol 84:426–436. https://doi.org/10.1128/jvi.00725-09
78. Zhao C, Hsiang TY, Kuo RL, Krug RM (2010) ISG15 conjugation system targets the viral NS1 protein in influenza A virus-infected cells. Proc Natl Acad Sci U S A 107:2253–2258. https://doi.org/10.1073/pnas.0909144107
79. Luo H (2016) Interplay between the virus and the ubiquitin-proteasome system: molecular mechanism of viral pathogenesis. Curr Opin Virol 17:1–10. https://doi.org/10.1016/j.coviro.2015.09.005
80. Querido E, Blanchette P, Yan Q et al (2001) Degradation of p53 by adenovirus E4orf6 and E1B55K proteins occurs via a novel mechanism involving a Cullin-containing complex. Genes Dev 15:3104–3117. https://doi.org/10.1101/gad.926401
81. Schwefel D, Boucherit VC, Christodoulou E et al (2015) Molecular determinants for recognition of divergent SAMHD1 proteins by the lentiviral accessory protein Vpx. Cell Host Microbe 17:489–499. https://doi.org/10.1016/j.chom.2015.03.004
82. Franck N, Le Seyec J, Guguen-Guillouzo C, Erdtmann L (2005) Hepatitis C virus NS2 protein is phosphorylated by the protein kinase CK2 and targeted for degradation to the proteasome. J Virol 79:2700–2708. https://doi.org/10.1128/jvi.79.5.2700-2708.2005
83. Kamio M, Yoshida T, Ogata H et al (2004) SOC1 inhibits HPV-E7-mediated transformation by inducing degradation of E7 protein. Oncogene 23:3107–3115. https://doi.org/10.1038/sj.onc.1207453
84. Ratia K, Kilianski A, Baez-Santos YM, Baker SC, Mesecar A (2014) Structural basis for the ubiquitin-linkage specificity and deISGylating activity of SARS-CoV papain-like protease. PLOS Pathog 10(5):e1004113. https://doi.org/10.1371/JOURNAL.PPAT.1004113
85. Álvarez E, DeDiego ML, Nieto-Torres JL et al (2010) The envelope protein of severe acute respiratory syndrome coronavirus interacts with the non-structural protein 3 and is ubiquitinated. Virology 402:281–291. https://doi.org/10.1016/j.virol.2010.03.015
86. Wang Q, Li C, Zhang Q et al (2010) Interactions of SARS coronavirus nucleocapsid protein with the host cell proteasome subunit p42. Virol J 7:1–8. https://doi.org/10.1186/1743-422X-7-99
87. Sojka D, Šnebergerová P, Robbertse L (2021) Protease inhibition—an established strategy to combat infectious diseases. Int J Mol Sci 22(11):5762. https://doi.org/10.3390/IJMS22115762
88. Sterz J, von Metzler I, Hahne JC et al (2008) The potential of proteasome inhibitors in cancer therapy. Expert Opin Investig Drugs 17:879–895. https://doi.org/10.1517/13543784.17.6.879
89. Raaben M, Posthuma CC, Verheije MH et al (2010) The ubiquitin-proteasome system plays an important role during various stages of the coronavirus infection cycle. J Virol 84:7869–7879. https://doi.org/10.1128/jvi.00485-10
90. Schneider M, Ackermann K, Stuart M et al (2012) Severe acute respiratory syndrome coronavirus replication is severely impaired by MG132 due to proteasome-independent inhibition of M-calpain. J Virol 86:10112–10122. https://doi.org/10.1128/jvi.01001-12
91. Wang J, Liang B, Chen Y et al (2021) A new class of α-ketoamide derivatives with potent anticancer and anti-SARS-CoV-2 activities. Eur J Med Chem 215:113267. https://doi.org/10.1016/J.EJMECH.2021.113267
92. Banerjee S, Wei T, Wang J et al (2019) Inhibition of dual-specificity tyrosine phosphorylation-regulated kinase 2 perturbs 26S proteasome-addicted neoplastic progression. Proc Natl Acad Sci U S A 116:24881–24891. https://doi.org/10.1073/PNAS.1912033116/-/DCSUPPLEMENTAL
93. Banerjee S, Ji C, Mayfield JE et al (2018) Ancient drug curcumin impedes 26S proteasome activity by direct inhibition of dual-specificity tyrosine-regulated kinase 2. Proc Natl Acad Sci U S A 115:8155–8160. https://doi.org/10.1073/PNAS.1806797115/-/DCSUPPLEMENTAL
94. Caputi FF, Di Cesare Mannelli L, Rullo L, et al (2020) The active second-generation proteasome inhibitor oprozomib reverts the oxaliplatin-induced neuropathy symptoms. Biochem Pharmacol 182:114255. https://doi.org/10.1016/J.BCP.2020.114255
95. Nguyen KT, Mun SH, Lee CS (2018) Hwang CS (2018) Control of protein degradation by N-terminal acetylation and the N-end rule pathway. Exp Mol Med 507(50):1–8. https://doi.org/10.1038/s12276-018-0097-y
96. Leleu X, Martin TG, Einsele H et al (2019) Role of proteasome inhibitors in relapsed and/or refractory multiple myeloma. Clin Lymphoma, Myeloma Leuk 19:9–22. https://doi.org/10.1016/j.clml.2018.08.016
97. Curran MP, McKeage K (2009) Bortezomib: a review of its use in patients with multiple myeloma. Drugs 69:859–888. https://doi.org/10.2165/00003495-200969070-00006
98. FDA (2003) VELCADE® (bortezomib) for injection, for subcutaneous or intravenous use. In: Accessdata.fda.gov. https://www.accessdata.fda.gov/drugsatfda_docs/label/2008/021602s015lbl.pdf
99. Shirley M (2016) Ixazomib: first global approval. Drugs 76:405–411. https://doi.org/10.1007/s40265-016-0548-5
100. Demo SD, Kirk CJ, Aujay MA et al (2007) Antitumor activity of PR-171, a novel irreversible inhibitor of the proteasome.

Cancer Res 67:6383–6391. https://doi.org/10.1158/0008-5472.CAN-06-4086
101. Groen K, Van de Donk NWCJ, Stege CAM et al (2019) Carfilzomib for relapsed and refractory multiple myeloma. Cancer Manag Res 11:2663–2675. https://doi.org/10.2147/CMAR.S150653
102. Obrist F, Manic G, Kroemer G, Vitale I, Galluzzi L (2015) Trial watch: proteasomal inhibitors for anticancer therapy. Mol Cell Oncol 2(2):e974463–1. https://doi.org/10.4161/23723556.2014.974463
103. Zhu H, Wang T, Xin Z et al (2019) An oral second-generation proteasome inhibitor oprozomib significantly inhibits lung cancer in a p53 independent manner in vitro. Acta Biochim Biophys Sin (Shanghai) 51:1034–1040. https://doi.org/10.1093/abbs/gmz093
104. Ng YL, Salim CK, Chu JJH (2021) Drug repurposing for COVID-19: approaches, challenges and promising candidates. Pharmacol Ther 228:107930. https://doi.org/10.1016/j.pharmthera.2021.107930
105. Pushpakom S, Iorio F, Eyers PA et al (2018) Drug repurposing: progress, challenges and recommendations. Nat Publ Gr. https://doi.org/10.1038/nrd.2018.168
106. Serafin MB, Bottega A, Foletto VS et al (2020) Drug repositioning is an alternative for the treatment of coronavirus COVID-19. Int J Antimicrob Agents 55:1–4. https://doi.org/10.1016/j.ijantimicag.2020.105969
107. Harris MJCAIJLMARFKM (2004) The Gene Ontology (GO) database and informatics resource. Nucleic Acids Res 32:258–261. https://doi.org/10.1093/nar/gkh036